

Received March 3, 2022, accepted March 23, 2022, date of publication March 28, 2022, date of current version April 27, 2022.

Digital Object Identifier 10.1109/ACCESS.2022.3162843

Modeling of Ship Encounter Risk Based on Riemann Sphere Projection Transformation

SHUZHEN CHEN^{1,2}, BIAO GONG¹, CHENG XIE^{1,2}, CHENGYONG LIU^{1,2}, ZHAO LIU^{1,2}, AND RUI WANG³

¹School of Navigation, Wuhan University of Technology, Wuhan 430062, China

²Hubei Key Laboratory of Inland Shipping Technology, Wuhan 430063, China

³Wuhan Hai Zhi Cheng Technology Company Ltd., Wuhan 430014, China

Corresponding author: Cheng Xie (cxie@whut.edu.cn)

This work was supported by the National Natural Science Foundation of China under Grant 52171351.

ABSTRACT With the continuous development of the shipping industry, the shipping traffic density is increasing day by day, and the ship collision accidents are increasing year by year. As the collision of ships will lead to serious losses, people pay more attention to how ships perceive the encounter risks and adopt safer navigation strategies. In order to quantify the risks in the process of ship encounter, this paper proposes a ship encounter risk perception model based on Riemann sphere projection transformation, which projects the relative motion trajectory of Ship as the relative curve motion on the Riemann sphere, constructs the encounter risk model by using the relative velocity and relative distance of the ship on Riemann sphere, and simulates it based on three encounter situations and actual accident cases, and compares the reliability of the model with the traditional fuzzy comprehensive evaluation model based on cases. The results show that the model proposed in this paper can effectively assess the ship encounter risks and creates a more intuitive real-time visual output, which is convenient to assist Ship Anti-collision decision-making. At the same time, it can provide theoretical basis for the inversion of ship collision accidents and the identification of responsibilities.

INDEX TERMS Encounter risk, Riemann sphere, projection transformation, visual output.

I. INTRODUCTION

In recent years, with the increasing number of ships, the density of ships at sea continues to increase, and the encounter situation between ships becomes more and more complicated. Although some NAVAIDS (Navigational Aids) have been developed, it is still impossible to measure the encounter risks between ships completely and accurately. For intelligent ships, real-time quantitative analysis and prediction of ship encounter risks is the premise of developing intelligent navigation technology and autonomous navigation collision avoidance technology. In the face of complicated ship encounter situations that change with time and space, how to make intelligent ships quantitatively perceive the encounter risks between ships and then take corresponding anti-collision decisions has become the key of current research on ship encounter and collision risks.

The associate editor coordinating the review of this manuscript and approving it for publication was Xi Wang Dong.

The first problem to be solved to realize autonomous navigation of ships is how to perceive the ship encounter risks and output digital signals for final anti-collision decision. At present, the perception of ship collision risk is mainly based on the quantitative assessment of ship collision risk and the risk threshold to judge the degree of ship collision risk. Scholars at home and abroad have done a lot of research work. The vast majority of scholars mainly focus on the geometric characteristics between own ship and other encounter ships to determine the hazard level, using DCPA and TCPA as the input variables without causality [1]–[3], using fuzzy theory [4]–[6], evidence theory [7]–[9], integrated consideration of ship domain [10]–[12] and other methods to calculate the collision hazard of ships, which cannot accurately grasp the weight relationship between TCPA and DCPA in nautical practice, and different criteria exist for their quantification, and their results are more subjective and The deviation is large. Fiorini *et al.* put forward the concept of velocity obstacle [13] in 1998, where, by calculating and controlling velocity, the velocity obstacle method is combined with ship

dynamics [14], the influence of external environment such as wind, waves, currents and ship dynamics is comprehensively considered [15], and nonlinear velocity obstacle is adopted [16], [17] for ship anti-collision, etc. These methods calculate whether own ship has collision risk according to the real-time relative velocity, so as to adjust the direction of relative velocity to avoid dynamic or static obstacles. The magnitude of the risk cannot be judged intuitively, and the final consequences that will be caused by each change backward are not further discussed. Mendel *et al.* put forward a projection risk model [18], [19], using Riemann sphere for spatial projection, the ship track is projected from sea level to the northern hemisphere of Riemann sphere, and the ship encounter risk is defined as the projection quantization value related to the ship spacing. This method can roughly reflect the size of risk, but only considers the influence of relative distance, ignoring the influence of relative velocity in visual risk perception, and there is a certain error in the accuracy of risk assessment. At the same time, the ship track is projected in the northern hemisphere of Riemann sphere, which can not fully reflect the projection correlation between the ship track moving at sea level and the curve projected on Riemann sphere. Through the above analysis, most of the existing studies discuss the encounter risk of ships in two-dimensional Euclidean space, which cannot fully reflect the general law of risk evolution in the process of ships encounter, and the potential impacts of each maneuvering operation are not lucubrated enough. At the same time, in the process of defining the final risk, there are many evaluation indicators and there is no uniform standard for the determination of the indicator weight.

In order to solve the above mentioned problems, this paper proposes an improved method to modeling and determining the ship encounter risk. Firstly, the defects of ship encounter risk assessment in the traditional Euclidean space are introduced, then, based on the projection of human vision, a ship encounter risk model based on Riemann sphere projection transformation is proposed, and the reliability of the model is verified by the risk evolution law of different encounter situations. Then, based on the actual ship collision accident case in a certain sea area, this model is used for accident replay inversion and responsibility analysis, and compared with the risk output of the traditional fuzzy comprehensive evaluation model. Finally, this model is used to analyze the evolution of ship encounter risk in multi-ship encounter situations.

This paper realizes the transformation from two-dimensional space to three-dimensional space, the evaluation index of the final risk definition adopts the relative speed and relative distance under the Riemannian sphere, takes the relative change rate as the weight, abandons the traditional multi index calculation of fuzzy comprehensive evaluation, and realizes the unity of index weight. It enables a more intuitive output of ship encounter risks more in accordance with the general law of the evolution of ship encounter risks. Through comprehensive analysis of the potential impact of each maneuvering operation on the ship, it can give early

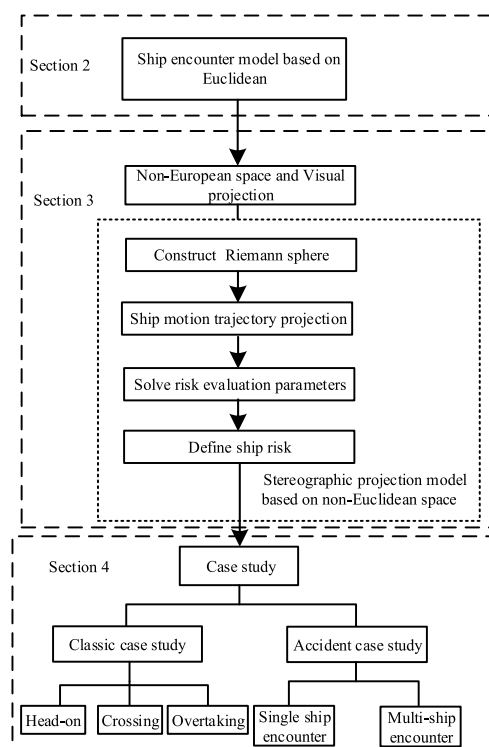


FIGURE 1. Technical Roadmap of this paper.

warning of potential collision risks in the process of ship encounters, and give a reasonable maneuver plan, which is of great significance to ensure the safety of ship navigation. At the same time, the model can deeply mine historical data to provide theoretical support for accident reconstruction inversion and accident liability identification, which is of great significance to maritime development. The technical roadmap of this paper is shown in Fig.1.

II. SHIP ENCOUNTER MODEL BASED ON EUCLIDEAN SPACE

A. SHIP MOTION MODEL IN EUCLIDEAN SPACE

The Euclidean space [20], [21] is a generalization of the studied 2D and 3D space in mathematics. This generalization transforms Euclid's concept of distance, length and angle into a coordinate system of any number of dimensions. Euclidean space is planar in nature and belongs to two-dimensional plane space.

It is assumed that before the anti-collision decision is made, the two ships are basically in the state of keeping a velocity and direction. Taking *Ship_A* as the coordinate origin, the due north direction as the *y* axis and the due east direction as the *x* axis, the ship encounter model in Euclidean space is established, as shown in Fig.2. The meanings of parameters in Fig. 2 are shown in Table 1.

The superposition principle of velocity is used to superimpose the motion velocity of own ship (*Ship_A*) onto the other ships (*Ship_B*), as shown in Fig. 2. *Ship_A* is considered to be at rest at this point and *Ship_B* is moving on the line *l*

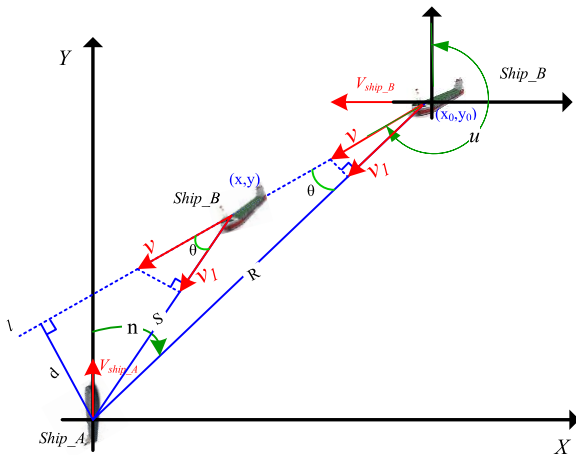


FIGURE 2. Ship encounter situation model in Euclidean space.

TABLE 1. Description of parameters of Euclidean space ship encounter model.

Parameter	Meaning description	unit
V_{ship_A}, V_{ship_B}	speed of ship_A and ship_B	knot
d	DCPA	n mile
v	resultant velocity of two ships	knot
v_1	relative velocity of two ships	knot
R	initial distance between two ships	n mile
S	the relative distance between two ships	n mile
μ	clockwise angle between Y axis and v	angle (°)
n	clockwise angle between the Y axis and the connecting line of two ships	angle (°)

with velocity v and initial distance between the two boats is R . The position coordinates (x, y) for the coordinates of the initial point (x_0, y_0) at the moment t in the coordinate system $Ship_A$ are expressed as follows:

$$\begin{cases} (x_0, y_0) = (R \sin(n), R \cos(n)) \\ x = x_0 + vt \times \sin(u) \\ y = y_0 + vt \times \cos(u) \end{cases} \quad (1)$$

Therefore, we can take any ship as own ship, analyze the movement process of other ships in the coordinate system centered on own ship, and analyze the encounter risks of ships.

B. ENCOUNTER RISK ANALYSIS IN EUCLIDEAN SPACE

The perception of encounter risk is often measured by the relative velocity and distance between own ship and target ships, which shows that the perceived collision risk should become larger and larger as the two ships approach each other. In the Euclidean space, the relative distance S can be obtained from Eq.(2), and it can be easily seen that the relative distance S gradually decreases with the increase of t (the two ships

gradually approach).

$$S = \sqrt{d^2 + (v \times TCPA - vt)^2} \quad (2)$$

The relative velocities v_1 of the two ships can be determined by the combined velocities v and θ as shown in Eq.(3).

$$v_1 = v \cos \theta = v \frac{v \times TCPA - vt}{\sqrt{d^2 + (v \times TCPA - vt)^2}} \quad (3)$$

The rate of change of the relative velocity v_1 is shown in Eq.(4), and it is obvious that $v'_1 < 0$, which indicates that the relative velocity of the two ships keeps decreasing in the process of constant approach.

$$v'_1 = \frac{(-1)v^2 d^2}{[d^2 + v^2(TCPA - t)^2]^{\frac{3}{2}}} \quad (4)$$

Therefore, in the Euclidean space, both the relative distance and the relative velocity gradually decrease with the increase of time t , which shows that in the Euclidean space, the two ships perceive that the velocity of the other side is getting smaller and smaller, and the risk perception will decrease with the decrease of velocity, which is obviously inconsistent with the actual situation. Under the condition of keeping the velocity and direction of the two ships, the risks perceived by the two ships should be larger and larger with the progress of the encounter process, and there are some defects in the risk assessment based on the Euclidean space ship encounter model alone.

III. CONSTRUCTION OF NON-EUCLIDEAN SPACE SPHERICAL PROJECTION MODEL

A. NON-EUCLIDEAN SPACE AND VISUAL PROJECTION

Non-Euclidean geometry [22] refers to geometric systems that differ from Euclidean geometry, referred to as non-Euclidean geometry, generally Riemannian geometry (hyperbolic geometry) and Riemannian elliptic geometry. The main difference between them and Euclidean geometry is that different parallel theorems are adopted in axiomatic system. In the Euclidean space, parallel lines will never intersect. However, in the non-Euclidean space, the object presents a feature where everything looks small in the distance and big on the contrary, that is, the parallel lines will gradually meet at a point in the distance, which reflects the most essential difference between Euclidean space and non-Euclidean space.

Vision projection or retinal imaging [23] is a method used by people to perceive the shape of external things. For our own visual projection imaging perception system, it belongs to the spherical space of non-European space. For ships, the relative motion trajectory of other ships is a straight line in Euclidean space (Fig.2) and a curve in human retina (Fig.4). The visual urgency perception of collision risk is intuitively reflected by the approaching of external things and the increase of relative velocity. The external environment is projected onto the drivers retina through the lens. Therefore, it is more in line with the objective law of facts to analyze

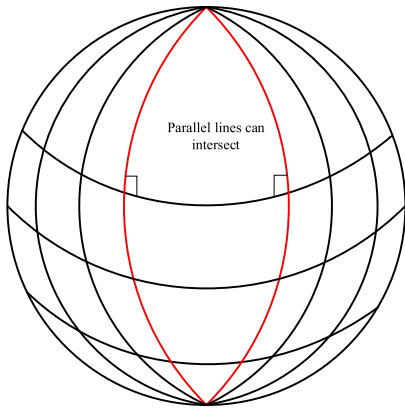


FIGURE 3. Non-Euclidean space described by Riemannian geometry.

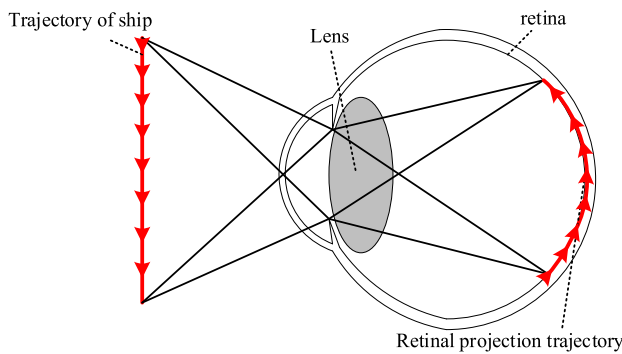


FIGURE 4. Projection of its relative motion trajectory on retina.

ship movements and encounter risks in non-Euclidean space with mathematical models.

Based on the principle of spherical imaging in non-Euclidean space, Riemann sphere is used as the basis of model construction. Based on the principle of projection transformation and non-Euclidean geometry [24], the spherical projection of the relative motion trajectory of other ships can transform the linear motion trajectory in Euclidean space into the curvilinear motion trajectory on the spherical surface of non-Euclidean space. The whole process is a conformal transformation in mathematics [25]. The specific process is as follows.

B. CONSTRUCTION RIEMANN SPHERE

Ship domain model is widely used in ship collision avoidance analysis. From 1960s to 1970s, the concept of ship domain was put forward [26], which was defined as “the domain around the previous ship the vast majority of subsequent ship pilots will avoid intruding into”. After that, many scholars conducted extensive research around this definition [27], [28]. In this paper, we construct own ship’s ship domain by taking *Ship_A* as the south pole of the Riemann sphere and on the basis of the ship length of *Ship_A*, and construct the Riemann sphere tangent to the sea level with the same radius as the radius *r* (5 times the length of the ship) of own ship’s ship domain. The coordinate system in

non-Euclidean space constructed under Riemann sphere is shown in Fig.5.

Where points *M* are the center of the sphere, points *O* are the Riemann sphere vertices (north pole). *Ship_B* The initial coordinates under the coordinate system are $(x_0, y_0, 0)$, and the coordinates of point *t* at the next moment are $(x, y, 0)$, and x_0, y_0, x, y is obtained from Eq. (1), and *l* is the relative motion trajectory of *Ship_B*, and the Riemann sphere with the expression shown in Eq. (5).

$$x^2 + y^2 + (z - r)^2 = r^2 \tag{5}$$

where, *r* is the Riemann sphere radius.

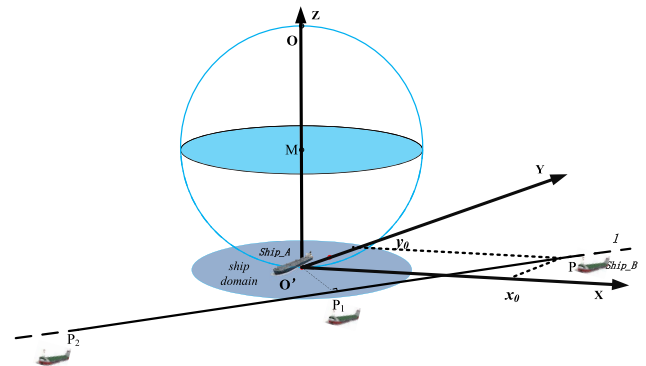


FIGURE 5. Construction of Riemann Sphere (Visual Projection Plane) Coordinate System.

C. PROJECTION OF SHIP TRAJECTORY BASED ON RIEMANN SPHERE

While *Ship_B* is moving on *l*, connects a position point $P(x, y, 0)$ for *Ship_B* running with the highest point $O(0, 0, 2r)$ of the Riemann sphere, forming the crossing *Q* on the sphere as shown in Fig.6, the straight line *OP* can be determined by two points *OP*, so that the crossing $Q(x, y, z)$ of the straight line *OP* with the Riemann sphere can be calculated.

$$\begin{cases} x = \frac{4r^2(-vt + R)}{(-vt + R)^2 + d^2 + 4r^2} \\ y = \frac{-4dr^2}{(-vt + R)^2 + d^2 + 4r^2} \\ z = \frac{2r^2[(-vt + R)^2 + d^2]}{(-vt + R)^2 + d^2 + 4r^2} \end{cases} \tag{6}$$

As is *OO'* the diameter of the Riemann sphere, the diameter is perpendicular to the sea level, it is easy to see that $\Delta O'OP$ is similar to $\Delta QOO'$, the projection point *P* at the Riemann sphere is the point *O'*, the projection point on the Riemann sphere on the sea level *Ship_A* is point *Q*. Therefore, the motion of *Ship_B* at the sea level relative to *Ship_A* can be projected as the motion of point *O'* on the Riemann sphere relative to point *Q*. The study of the variation relation of vector $O'Q$ in non-Euclidean space can be considered as equivalent to the study of the motion relation of *Ship_B* relative to *Ship_A* in Euclidean space. The projection of the

combined velocity v in Euclidean space onto non-Euclidean space is v' , the projection of v' on the vector $\vec{O'Q}$ is the relative velocity $V_{\vec{OQ}}$ of the two ships in non-Euclidean space, and the length of the vector $\vec{O'Q}$ is the relative distance S between the two ship. When *Ship_B* starts moving at l from infinity, a segment of arc is projected on the Riemann sphere as shown in Fig.7. Therefore, the Euclidean spatial characteristics of the encounter between two ships at sea level will be transformed into non-European spatial characteristics.

Table 2 shows the transformation table of parameters between Euclidean space and Riemann sphere.

D. RISK ASSESSMENT OF SHIP ENCOUNTER

The relative distance S in Euclidean space is transformed by projection into S' , in non-Euclidean space, which is the norm of the vector \vec{OQ} , and the coordinates of the point Q can be found by formula (6). Thus the projected relative distance between the two ships is

$$S = \left| \vec{OQ} \right| = \sqrt{\frac{[4r^2(R - Vt)]^2 + 16d^2r^4 + 4r^4[(R - Vt)^2 + d^2]^2}{[(R - Vt)^2 + d^2 + 4r^2]^2}} \tag{7}$$

where, S is the projected relative distance.

The relative velocities in the Riemann sphere are

$$V_{\vec{OQ}} = \frac{\frac{dx}{dt} \times (-x(t)) + \frac{dy}{dt} \times (-y(t)) + \frac{dz}{dt} \times (-z(t))}{\sqrt{(-x(t))^2 + (-y(t))^2 + (-z(t))^2}} \tag{8}$$

where, $V_{\vec{OQ}}$ is the relative velocities. $x(t)$, $y(t)$ and $z(t)$ are the projection of the distance of the ship to the three directions of x , y , z over time.

According to COLREGS, it is generally considered that there is no collision risk when overtaking situations are more than 3nmile apart and head-on situations are more than 6nmile apart. For a ship at infinity, the projected point of its Riemann sphere is infinitely close to the North Pole, so the diameter of the Riemann sphere is used as the maximal

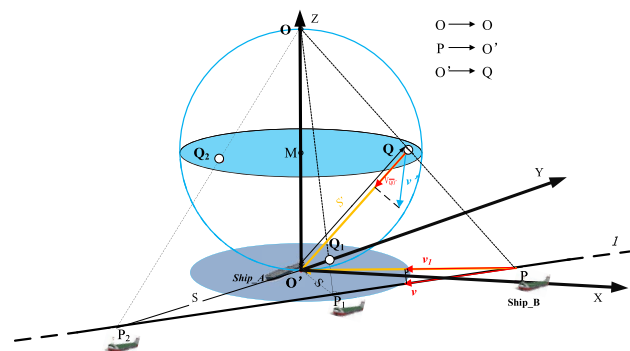


FIGURE 6. Ship projection transformation model based on similarity principle.

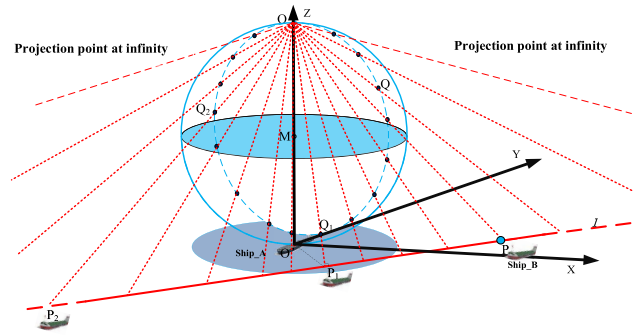


FIGURE 7. Trajectory projection transformation process.

TABLE 2. Parameter correspondence table.

	Euclidean space	Riemann sphere
trajectory	l	arc(OOQ_1Q_2O)
target ship coordinate	P, P_1, P_2	Q, Q_1, Q_2
resultant velocity	v	v'
relative velocity	v_l	$V_{\vec{OQ}}$
relative distance	S	S'

value S_{max} of the projected relative distance, and the minimal value S_{min} of the projected relative distance is 0 when the two ships collide (the minimum encounter distance is 0). The relative distance decreases and the quantization value of relative distance increases gradually during the process of ships' continuous approach.

$$S_r = \frac{S_{max} - S}{S_{max} - 0} \tag{9}$$

where, S_r is the normalized relative distance.

For relative velocity, the greater the relative velocity of projection, the greater the perceived risk of encounter. Since the relative velocity between ships is generally less than 30 knots in the conventional state, the maximal value of the relative velocity after converting the combined velocity of 30 knots into the Riemann sphere is taken as V_{max} , and then the relative velocity is normalized V_r as:

$$V_r = \frac{V_{\vec{OQ}} - 0}{V_{max} - 0} \tag{10}$$

When combining the effects of each evaluation index factor, in order to evaluate more effectively, the evaluation factors should be combined using the additive or multiplicative rule [29], and the general expression is $R_{risk} = \sum_{i=1}^n w_i y_i$.

$R_{risk} = \sum_{i=1}^n w_i y_i$ or $R_{risk} = \prod_{i=1}^n y_i$, where w are the corresponding weights of the evaluation parameters and y are the evaluation parameters. For the Riemann sphere projection transformation model, relative velocity and relative distance affect the risk together. This paper comprehensively evaluates the risk in the form of addition. Take the rate of change of relative velocity and relative distance as a measure of their

contribution rate to risk change, and normalize them as their respective weights. The quantification of collision risk is shown in formulas (11) and (12).

$$\begin{cases} W_s = \frac{\frac{dS_r}{dt}}{\left| \frac{dS_r}{dt} \right| + \left| \frac{dV_r}{dt} \right|} \\ W_v = \frac{\frac{dV_r}{dt}}{\left| \frac{dS_r}{dt} \right| + \left| \frac{dV_r}{dt} \right|} \end{cases} \quad (11)$$

$$R_{risk} = W_s \times S_r + W_v \times V_r \quad (12)$$

Among them, W_s is the weight of relative distance; W_v is the weight of relative velocity, R_{risk} is the calculated value of ship encounter risk.

IV. CASE STUDY

A. CLASSICAL ENCOUNTER SITUATION RESEARCH

Misganaw Abebe [8] et al. put forward a new method to calculate risks by combining machine learning with D-S theory, and summarized the evolution of risks in three situations: crossing encounter, head-on encounter and overtaking encounter. The results show that with the approaching of the two ships, the risk of encounter between the two ships gradually increases. Under the same external conditions, the risk basically shows as follows: head-on encounter risk > crossing encounter risk > overtaking encounter risk. Based on this, this paper also analyzes the evolution of ship encounter risk under the Riemann sphere projection transformation model, aiming at three situations of crossing encounter, head-on encounter and overtaking. In addition, due to the difference in risk perception among ships of different sizes, the influence of different sizes of ships on risk perception under three encounter situations based on COLREGS is compared in order to explore the law, as shown in Fig. 8.

The input value (R, V, L, n, u) of the model for the validation process is obtained by transforming the data of latitude and longitude, heading and navigational velocity of the two ships via the Euclidean spatial model in Chapter 2, for the convenience of calculation. Therefore, two ships of different sizes, A and B, are set up to study the three situations of crossing, head-on and overtaking encounter respectively. In the same situation, we study the A and B ships respectively, that is, superimpose the combined velocity V of the two ships on the A or B ships in three situations respectively. When Ship A is the research object, that is, Ship A is own ship. At this time, the combined velocity V is superimposed on Ship B, and the input values of the risk model are shown in Table 3. Take Ship B as the research object, that is, B is own ship. At this time, the combined velocity V is superimposed on Ship A, and the input values of the encounter risk model are shown in Table 4. The encounter process of two ships is shown in Fig.9.

The initial calculated distance R of both ships is 3 nautical miles, in which Ship A length $L=200m$ and Ship B length $L=50m$. The data in Tables 3 and 4 are used as model inputs for the three encounter scenarios using python, and the projected relative distances S_r , relative velocities V_r and

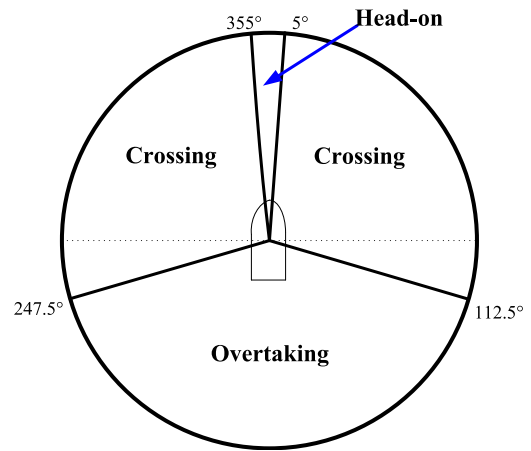


FIGURE 8. Ship encounter situation based on COLREGS.

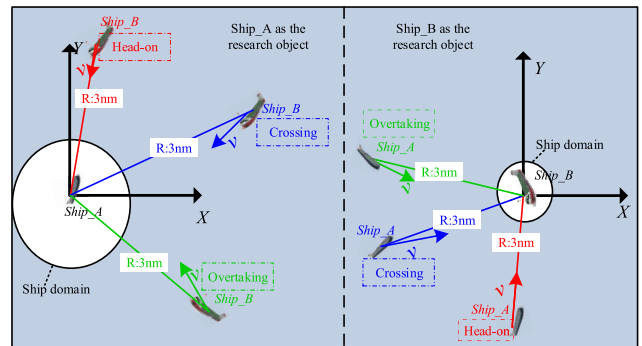


FIGURE 9. Ship encounter situation based on COLREGS.

risk values R_{risk} are calculated and visualized in the form of tracing points, provided that the ships take the direction and velocity preservation. In each encounter situation calculation, the moment when both ships move from 3 nautical miles apart to the collision point (moment of intrusion into the ship’s domain) or the moment when both ships are exactly avoiding each other (moment of arrival at the DCPA). The results are shown in Fig.10, 11 and 12.

Fig.10, 11 and 12 respectively show the visualization results of ship encounter risks in three situations based on the model: head-on, crossing and overtaking encounter. The left diagrams of Fig.10, 11 and 12 respectively show the changes of relative velocity and relative distance between Ship A and Ship B under three kinds of encounter situations, and the right diagrams respectively show the changes of encounter risks. When the two ships move by keeping a velocity and direction from 3 nautical miles apart, the changing trend of the relative velocity and distance of the two ships gradually increases, and the risk of encounter between the two ships also gradually increases. As the two ships approach each other, the faster the risk increases, which is consistent with people’s intuitive perception of the risk of encounter (the closer the distance, the greater the velocity and the higher the risk).

On the whole, before invading the other ship’s domain, ships of different sizes have different perceptions of risks,

and the degree of risk perception of Ship A is obviously greater than that of Ship B. The reason is that ships construct Riemann spheres based on their respective captains and the diameters of Riemann spheres are different, so the spatial positions of the ship's combined motion trajectories projected on different Riemann spheres are different, which leads to differences in their quantification, but this difference is more in line with navigation practice. At the same time, as can be seen from Fig. 10, 11 and 12, for different situations, if there is little difference in the distance and velocity between Ship A and Ship B, it will directly affect the quantization value of the combined velocity between ships as different encounter situations are mainly divided according to the gunwale angle. Therefore, it will eventually have a direct impact on the peak value of encounter risk, which generally shows as: head-on encounter risk > crossing encounter risk > overtaking encounter risk, which is consistent with Abebes research conclusion, and also conforms to the navigation practice.

TABLE 3. Input values of encounter risk model (Ship A as the research object).

encountering situations	R (n mile)	v (kn)	L (m)	n (°)	μ (°)
Crossing	3	14.16	200	73.97	246.23
Heading on	3	23.46	200	4.2	184.2
Overtaking	3	5.17	200	126.28	330.32

TABLE 4. Input values of encounter risk model (Ship B as the research object).

encountering situations	R (n mile)	v (kn)	L (m)	n (°)	μ (°)
Crossing	3	14.16	50	253.97	46.23
Heading on	3	23.46	50	184.2	4.2
Overtaking	3	5.17	50	306.28	150.32

B. ACCIDENT CASE ANALYSIS

In order to further verify the reliability of the model, a case of collision accident in a certain sea area was selected as

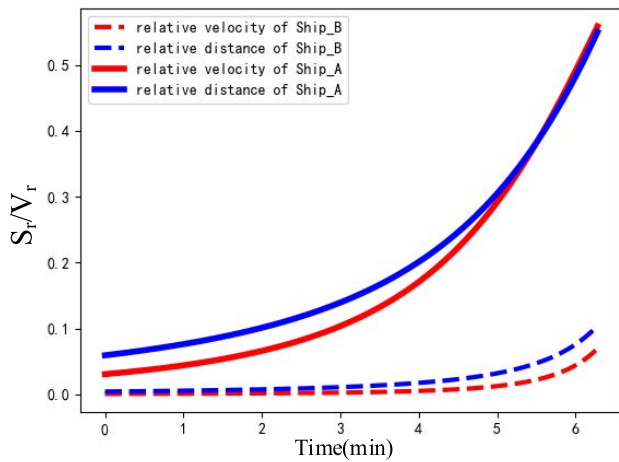


FIGURE 10. S_r, V_r, R_{risk} under Head-On encounter.

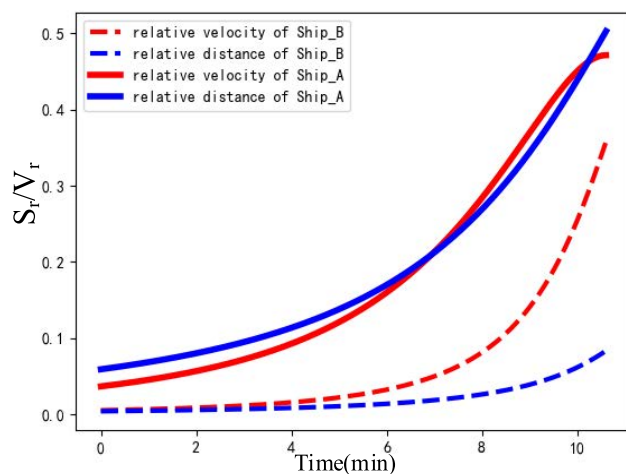
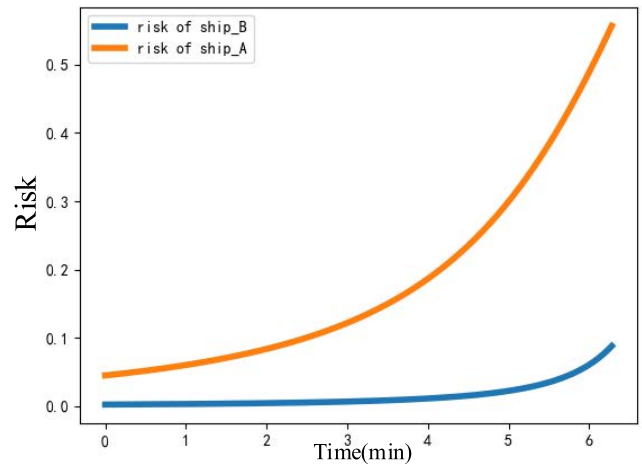
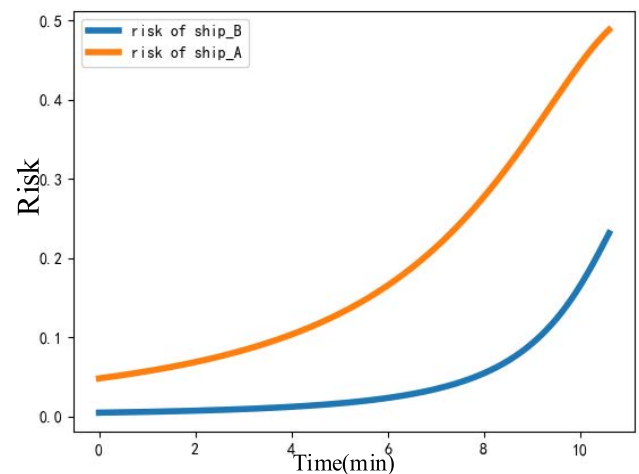


FIGURE 11. S_r, V_r, R_{risk} under crossing encounter.



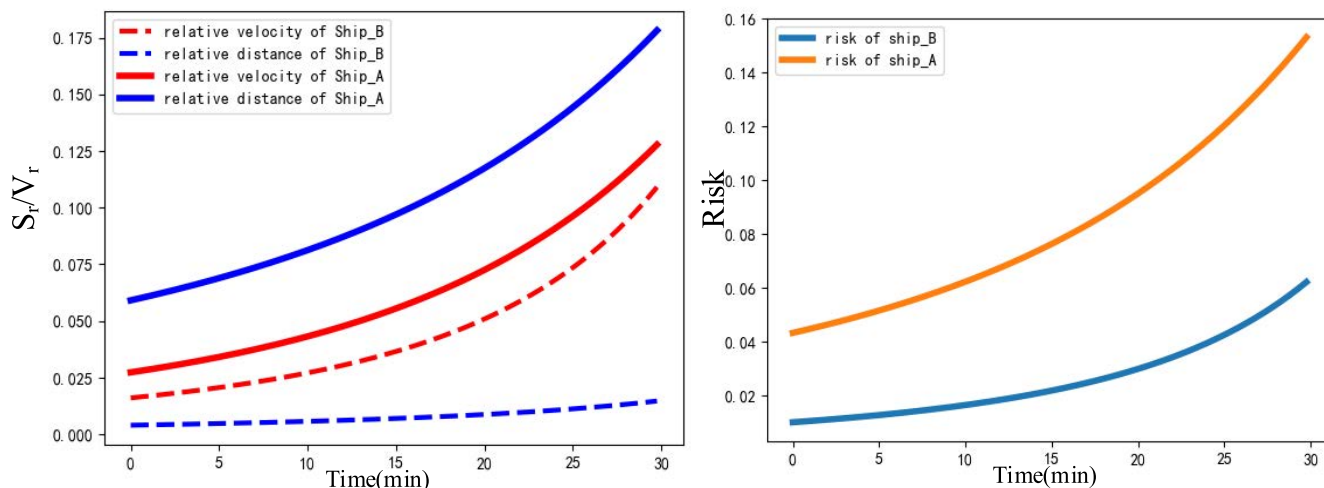


FIGURE 12. S_r, V_r, R_{risk} under overtaking encounter.

the research object. The accident occurred at 4: 00 a.m. on a certain day, when the container freighter “A” left Dongying Port, it collided with the dry bulk freighter “B” in the waters near Dongying Port with latitude and longitude coordinates of 38°2’ 48’’N and 119°1’ 26’’E. The accident caused local deformation and damage of the middle and rear body at the left larboard of Ship B. The bulbous bow of Ship “A” is deformed and damaged, and the tip cabin is flooded, causing no water pollution or death. The collision process reconstructed based on historical data is shown in Fig. 13.

Table 5 shows the AIS data of the accident ships (Ship A and B) after finishing the encounter process, and the encounter process lasts 10.77 minutes. Before this collision accident, the two ships carried out three maneuvers in total. At 4min, Ship B slowed down and turned right, at 5min, Ship A slowed down and turned right, at 9min, Ship A accelerated and turned right, and at 10.77min, the two ships collided.

Firstly, the accident ship is analyzed separately. In order to compare with Riemann sphere projection transformation model, the classical fuzzy comprehensive evaluation model is selected. Fuzzy model applies comprehensive evaluation theory in fuzzy mathematics, taking five basic parameters of target ship’s distance, relative bearing, nearest encounter distance, time to nearest point and ship velocity ratio as evaluation parameters of collision risk degree. By determining the membership function of each parameter, the weighted sum of membership function values of each parameter is used as the final risk evaluation basis. The AIS data of the accident ship in table 5 is converted into some input data based on the fuzzy collision risk model as shown in table 6.

Based on the data in Table 6, the encounter hazard of Ship A at each moment is calculated, and the expressions are $E = a_{DCPA}f_{DCPA} + a_{TCPA}f_{TCPA} + a_{DFD} + a_Bf_B + a_kf_k$, and a are the weights of each indicator. where the value of each weight [29]: $a_{DCPA} = 0.36, a_{TCPA} = 0.32, a_D = 0.14, a_B = 0.10, a_k = 0.08, f$ is the affiliation function of

each indicator [30], [31]. Finally, the change of risk degree with time will be visually output, as shown in Fig. 14.

Taking the 200m container ship as the research object (own ship), the AIS data is transformed into input data of ship encounter model based on Riemann sphere projection transformation, as shown in Table 7.

According to the data in Table 7, the ship encounter model based on Riemann sphere projection transformation calculates the change of the relative distance of encounter situation with time as shown in Fig. 15, and the change of encounter risk with time as shown in Fig. 16.

Then, taking Ship A among the accident ships as the research object, the Riemann sphere projection transformation model is used to analyze the risk evolution between all the ships it will encounter during the accident, and the real-time visual output is made. The results are shown in Fig. 17.

Where, risk of ship_B, Risk of ship_C and Risk of ship_D are ship_A perceived the risk of the surrounding ships before the accident, and the collision point is the perceived risk of the accident between ship_A and ship_B.

C. DISCUSSION OF RESULTS

As can be seen from Fig. 14, Fig. 15 and Fig. 16, the two accident ships have carried out three times of change operations in velocity and direction. Fig. 14 shows the change of real-time relative distance (solid line) and predicted relative distance (dashed line) of two ships’ encounter time with time. Judging from the predicted value of the final relative distance, all maneuvers can’t avoid Ship A, that is, all maneuvers reach the quantified value of the safe distance of 0.54 (the projected quantified value of the safe distance on Riemann sphere) in Fig. 14. Only from the change trend of relative distance, the time to reach the safe distance predicted in the second stage is the longest, which shows that the first maneuvering operation (deceleration and right turn of Ship B) is the most effective

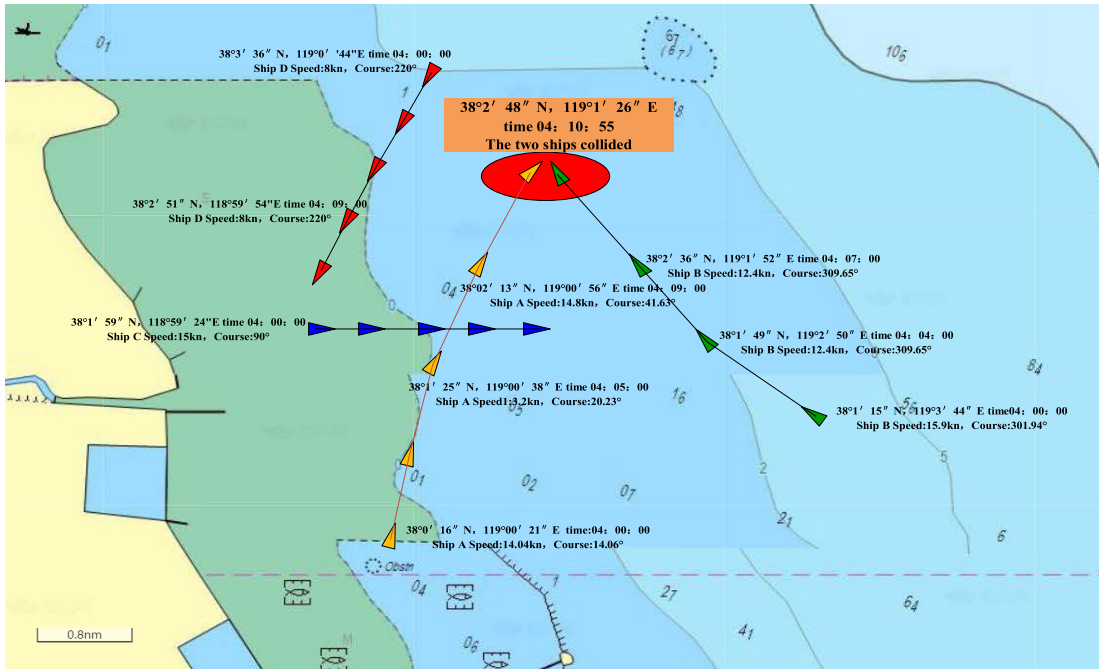


FIGURE 13. Ship crossing accident process.

TABLE 5. AIS data of accident ship.

Stage	Ship_A					Ship_B				
	Time	Latitude	Longitude	Speed	Heading	Latitude	Longitude	Speed	Heading	
I	04:00:00	38°00'16"N	119°00'21"E	14.04	14.06	38°01'15"N	119°03'44"E	15.9	301.94	
II	04:04:00	38°00'23"N	119°00'21"E	14.04	14.06	38°01'49"N	119°02'50"E	12.4	309.65	
III	04:05:00	38°01'25"N	119°00'38"E	13.2	20.23	38°01'58"N	119°02'38"E	12.4	309.65	
IV	04:09:00	38°01'49"N	119°00'38"E	14.8	41.63	38°02'36"N	119°02'14"E	12.4	309.65	

compared with the other two operations, which accords with the practice of preventing collisions at sea, and further illustrates the rationality of this model.

Fig.14 and Fig.16 respectively show the visualization results of the traditional fuzzy comprehensive evaluation model and the Riemann sphere projection transformation model for the encounter risks of two ships. The two models have the same overall trend of risk evaluation, and the sudden change trend of risk caused by each change operation in velocity and direction of the two models is the same, which shows that the instantaneous risk of the first and third velocity change increases, and the instantaneous risk of the second velocity change decreases, which is identical. There are some differences in the evaluation of risks in individual stages. The main reason is that the weights and auxiliary parameters of each factor in traditional fuzzy comprehensive evaluation model mostly come from empirical data or statistical data, and there are differences in the membership functions of the risk degree of each factor, which are not necessarily

TABLE 6. Input values based on fuzzy collision risk model.

Time (min)	DCPA (n mile)	TCPA (min)	Distance (D) (n mile)	Direction (B) (degree)	Speed ratio (K)
0	0.117	11.937	3.52	74.04	0.883
4	0.356	9.800	2.34	73.97	1.13
5	0.117	8.541	2.11	75.58	1.68
9	0.054	3.412	1.12	77.99	1.194

completely in line with the current actual situation and are kind of subjective, and the output of the model changes linearly with large errors. However, the risk evaluation based on the Riemann sphere projection transformation model is completely in accordance with the objective AIS data, and the output of the model changes nonlinearly. The closer the two ships get to the collision point, the faster the risk will increase, which is in line with people’s basic perception. It can not only achieve real-time output, but also quickly predict the subsequent risk changes, and also intuitively evaluate the consequences of each maneuvering operation.

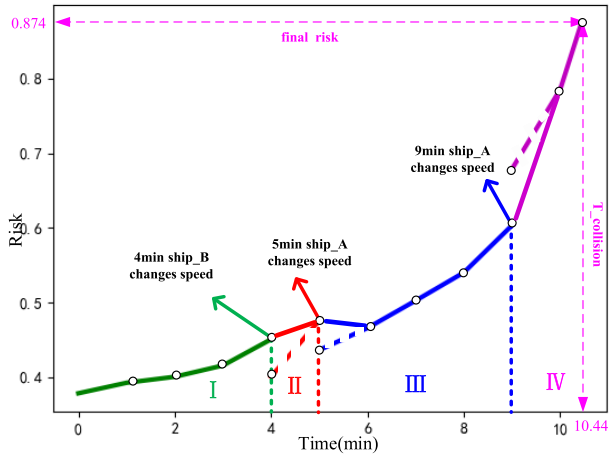


FIGURE 14. Visualization of ship collision risk based on fuzzy comprehensive evaluation.

TABLE 7. Input values of ship encounter model based on Riemann sphere projection transformation.

Time(min)	R(n mile)	V(kn)	L (m)	α (°)	μ (°)
0	3.52	17.69	200	74.04	252.88
4	2.34	14.16	200	73.97	246.23
5	2.11	14.80	200	75.58	252.41
9	1.12	19.63	200	77.99	260.77

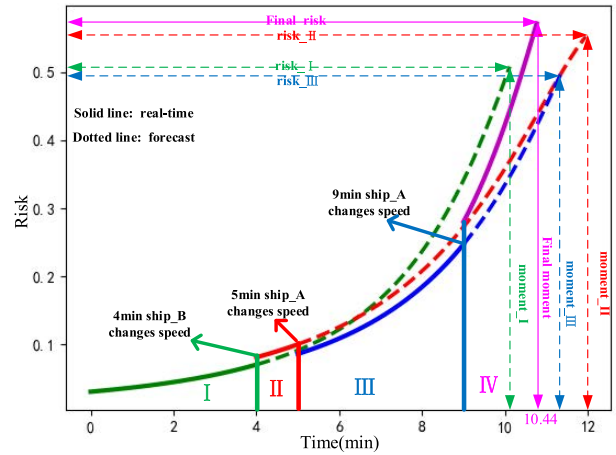


FIGURE 16. Visualization of risk of ship encounter situation.

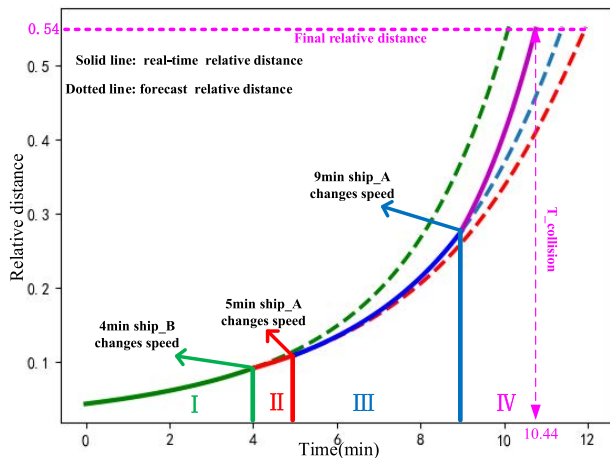


FIGURE 15. Visualization of relative distance of ship encounter situation.

As shown in Fig.16, at the moment of 4 minutes, Ship B slows down and turns right. Although this operation failed to reduce the peak risk of the two ships, compared with the initial stage, the immediate risk decreased at this moment, and the collision time was delayed by about 110.4 seconds, which is a favorable operation in terms of the risk of the two ships. At 5 minutes, Ship A slowed down and turned right, which led to the decrease of the immediate risk at that moment, and the peak risk of the two ships was decreased, but the collision time was slightly advanced by about 33.6 seconds, which needs further analysis on the whole. Nine minutes later, Ship A accelerated to turn right, which led to a sharp increase in immediate risk at that moment. At the same time, the peak

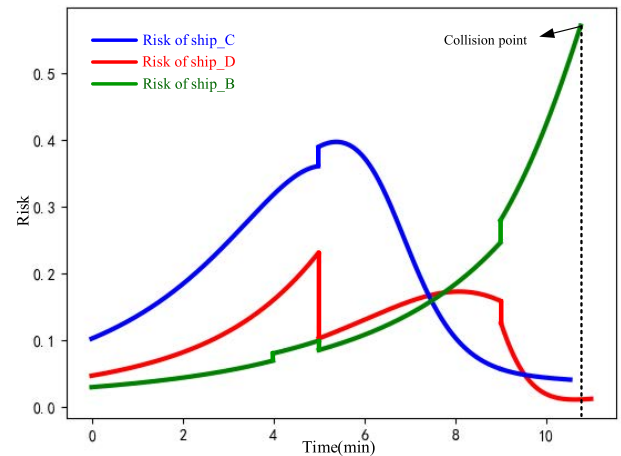


FIGURE 17. Ship A's Real-time risk perception.

risk of the two ships increased, and the collision time was advanced by about 37.8 seconds. Therefore, from the point of view of ship manipulation when two ships meet, the change operation in velocity and direction of Ship A at the moment of 9 minutes is the main factor leading to the final collision between the two ships, and in this case, Ship A should bear the main responsibility.

According to the real-time perceived risks of Ship A in Fig.17, the risks of other ships perceived by Ship A 5 minutes ago are shown as risks of Ship C risk > D Ship risk > Ship B risk, the perceived risk value of ship C is larger 1min about 5 minutes. Therefore, ship C is avoided by slowing down and turning right. The avoidance process lasts for about 1 minute, and then the risk of ship C is rapidly reduced. Ship D has always kept a relatively safe encounter distance, and the perceived risks are basically 8min a low range. After 8 minutes, the risks of both ships C and D are reduced. At this time, Ship A has successfully avoided ships C and D. 9minA changed direction again, and then did not take other actions, which made the risk with Ship B increase to the peak, and the risk reached the peak, that is, two ships collided. Under the

situation of multi-ship collision, the model can intuitively output the collision risks of other ships, can compare and analyze the risk evolution of each ship, and reasonably choose the collision avoidance time and the collision avoidance time, so as to help ships avoid collision.

To sum up, the output of this model accords with the basic navigation practice. Compared with the traditional model, this model completely depends on the objective change of relative velocity and relative distance, which avoids the interference of subjective factors on indexes and weights, and is more in line with people's intuitive perception. In addition, it is also possible to intuitively recognize the changes in the peak value and occurrence time of the encounter risks of two ships caused by the ship maneuvering at any time, and then quantitatively measure the impact of this maneuvering operation on the encounter risks of two ships, thus providing theoretical support for subsequent ship anti-collision decisions and accident liability determination. In the process of multi-ship encounter, we can clearly and intuitively judge the risks of other ships to our own ship, and determine the priority ships to avoid collision according to the magnitude of the risks, and judge the stage of ship encounter through the evolution of risks, which can help ships avoid collision.

V. CONCLUSION

This paper proposes ship encounter risk model based on Riemann sphere projection transform. Taking the whole Riemann sphere as the projection plane, the ship's relative linear motion in Euclidean space is transformed into relative curvilinear motion in non-Euclidean space by conformal transformation, and the ship's relative motion trajectory can be completely projected on the Riemann sphere, which reflects the consistency and continuity of similarity transformation and realizes the transformation from two-dimensional space to three-dimensional space. Finally, combined with the influence of relative velocity and relative distance on the ship encounter risks, it is used as the basis of risk assessment.

In this paper, three kinds of encounter situations between ships of different sizes, namely, head-on encounter, crossing encounter and overtaking encounter, are modeled, and the consistency between the output results of the model and navigation practice is verified. The model is applied to actual cases to analyze the risk evolution of collision accidents, and compared with the traditional fuzzy comprehensive evaluation model. The results show that the encounter model can continuously quantify the encounter risks of ships in different encounter situations, and make friendly visual output. The output results accord with the basic cognition of navigation practice and are consistent with the output of traditional fuzzy comprehensive evaluation model. Considering the parameters of human perception of encounter risks, the model only considers the comprehensive changes of two indicators, avoiding the detailed calculation of multi-objectives and weights in fuzzy comprehensive evaluation, and the output results are more in line with people's basic perception of encounter risks. At the same time, the output results realize

the monitoring and prediction of encounter risks, so that the pilot can form an intuitive perception of the changing trend of current maneuvering operation and encounter risks, and can have an intuitive perception of the risks of all surrounding ships, which can help the ship to make anti-collision decisions. In the process of accident inversion, It can provide theoretical basis for the evaluation of all maneuvering behaviors in time series, the detailed evaluation in the process of accident replay and inversion, and the identification of ship collision accident liability.

REFERENCES

- [1] C. Xie, J. Deng, Y. Zhuang, and H. Sun, "Estimating oil pollution risk in environmentally sensitive areas of petrochemical terminals based on a stochastic numerical simulation," *Mar. Pollut. Bull.*, vol. 123, nos. 1–2, pp. 241–252, Oct. 2017.
- [2] L. Kang, Z. Lu, Q. Meng, S. Gao, and F. Wang, "Maritime simulator based determination of minimum DCPA and TCPA in head-on ship-to-ship collision avoidance in confined waters," *Transportmetrica A, Transp. Sci.*, vol. 15, no. 2, pp. 1124–1144, 2019.
- [3] Y. Ren, J. Mou, Q. Yan, and F. Zhang, "Study on assessing dynamic risk of ship collision," in *Proc. Multimodal Approach Sustained Transp. Syst. Develop., Inf., Technol., Implement. (ICTIS)*, 2011, pp. 2751–2757.
- [4] S. S. Arici, E. Akyuz, and O. Arslan, "Application of fuzzy bow-tie risk analysis to maritime transportation: The case of ship collision during the STS operation," *Ocean Eng.*, vol. 217, Dec. 2020, Art. no. 107960.
- [5] Y. A. Ahmed, M. A. Hannan, M. Y. Oraby, and A. Maimun, "COLREGs compliant fuzzy-based collision avoidance system for multiple ship encounters," *J. Mar. Sci. Eng.*, vol. 9, no. 8, p. 790, Jul. 2021.
- [6] L. P. Perera, J. P. Carvalho, and C. G. Soares, "Intelligent ocean navigation and fuzzy-Bayesian decision/action formulation," *IEEE J. Ocean. Eng.*, vol. 37, no. 2, pp. 204–219, Apr. 2012, doi: [10.1109/JOE.2012.2184949](https://doi.org/10.1109/JOE.2012.2184949).
- [7] M. Abebe, Y. Noh, C. Seo, D. Kim, and I. Lee, "Developing a ship collision risk index estimation model based on Dempster–Shafer theory," *Appl. Ocean Res.*, vol. 113, Aug. 2021, Art. no. 102735.
- [8] Z. Shen and Q. Zhang, "Ship accident prediction model based on D-S evidence theory," in *Proc. IEEE 3rd Int. Conf. Civil Aviation Saf. Inf. Technol. (ICCASIT)*, Oct. 2021, pp. 818–821, doi: [10.1109/ICCA-SIT53235.2021.9633364](https://doi.org/10.1109/ICCA-SIT53235.2021.9633364).
- [9] L. Xiong, J. Tian, J. Zhou, and P. Shang, "A study of ship supportability evaluation using AHP and DS evidence theory," in *Proc. IEEE Int. Conf. Mechatronics Automat. (ICMA)*, Aug. 2021, pp. 1402–1406.
- [10] H. Namgung and J.-S. Kim, "Collision risk inference system for maritime autonomous surface ships using COLREGs rules compliant collision avoidance," *IEEE Access*, vol. 9, pp. 7823–7835, 2021, doi: [10.1109/ACCESS.2021.3049238](https://doi.org/10.1109/ACCESS.2021.3049238).
- [11] F. Deng, L. Jin, X. Hou, L. Wang, B. Li, and H. Yang, "COLREGs: Compliant dynamic obstacle avoidance of USVs based on the dynamic navigation ship domain," *J. Mar. Sci. Eng.*, vol. 9, no. 8, p. 837, Aug. 2021.
- [12] R. Szlapczynski, P. Krata, and J. Szlapczynska, "Ship domain applied to determining distances for collision avoidance manoeuvres in give-way situations," *Ocean Eng.*, vol. 165, pp. 43–54, Oct. 2018.
- [13] P. Fiorini and Z. Shiller, "Motion planning in dynamic environments using velocity obstacles," *Int. J. Robot. Res.*, vol. 17, no. 7, pp. 760–772, Jul. 1998.
- [14] P. Chen, M. Li, and J. Mou, "A velocity obstacle-based real-time regional ship collision risk analysis method," *J. Mar. Sci. Eng.*, vol. 9, no. 4, p. 428, Apr. 2021.
- [15] X. Yuan, D. Zhang, J. Zhang, M. Zhang, and C. G. Soares, "A novel real-time collision risk awareness method based on velocity obstacle considering uncertainties in ship dynamics," *Ocean Eng.*, vol. 220, Jan. 2021, Art. no. 108436.
- [16] Y. Huang, P. H. A. J. M. van Gelder, and Y. Wen, "Velocity obstacle algorithms for collision prevention at sea," *Ocean Eng.*, vol. 151, pp. 308–321, Mar. 2018.
- [17] P. Chen, Y. Huang, E. Papadimitriou, J. Mou, and P. H. A. J. M. van Gelder, "An improved time discretized non-linear velocity obstacle method for multi-ship encounter detection," *Ocean Eng.*, vol. 196, Jan. 2020, Art. no. 106718.

[18] M. Mendel, G. Reniers, and P. V. Gelder, "Risk in the safety sciences: Its economic foundations, its hyperbolic geometry, and its engineering methods," in *Proc. 25th Eur. Saf. Rel. Conf. (ESREL)*, 2015, pp. 1–6.

[19] M. Mendel and P. Van Gelder, "Visualizing and gauging collision risk," in *Proc. 26th Eur. Saf. Rel. Conf., Risk, Rel. Saf., Innov. Theory Pract.* Boca Raton, FL, USA: CRC Press, 2016, pp. 2877–2883.

[20] A. Darmochwał, "The Euclidean space," *Formalized Math.*, vol. 2, no. 4, pp. 599–603, 1991.

[21] S. Kakutani, "Some characterizations of Euclidean space," *Jpn. J. Math., Trans. Abstr.*, vol. 16, pp. 93–97, 1940.

[22] P. Ryan, *Euclidean and Non-Euclidean Geometry: An Analytic Approach*. Cambridge, U.K.: Cambridge Univ. Press, 1986.

[23] H. C. Longuet-Higgins and K. Prazdny, "The interpretation of a moving retinal image," *Proc. Roy. Soc. B, Biol. Sci.*, vol. 208, no. 1173, pp. 385–397, 1980.

[24] L. Henderson, *The Fourth Dimension and Non-Euclidean Geometry*. Princeton, NJ, USA: Princeton Univ. Press, 1983.

[25] L. Xu and H. Chen, "Conformal transformation optics," *Nature Photon.*, vol. 9, no. 1, pp. 15–23, 2015.

[26] Y. Fujii and K. Tanaka, "Traffic capacity," *J. Navigat.*, vol. 24, no. 4, pp. 543–552, 1971.

[27] A. Rawson and M. Brito, "Developing contextually aware ship domains using machine learning," *J. Navigat.*, vol. 74, no. 3, pp. 515–532, May 2021.

[28] T. Chai, J. Weng, and G. Li, "Estimation of vessel collision frequency in the Yangtze river estuary considering dynamic ship domains," *J. Mar. Sci. Technol.*, vol. 25, no. 3, pp. 964–977, Sep. 2020.

[29] J. Zhou and C. Wu, "Construction of the collision risk factor model," *J. Ningbo Univ.*, vol. 17, no. 1, pp. 61–65, 2004.



CHENG XIE received the M.Sc. and Ph.D. degrees from the Wuhan University of Technology, in 2015 and 2020, respectively. He is currently a Postdoctoral Researcher in traffic control and information engineering with the Wuhan University of Technology. His research interests include safety engineering and shipping pollution prevention.



CHENGYONG LIU received the M.Sc. and Ph.D. degrees from the Wuhan University of Technology, in 2006 and 2012, respectively. He is currently an Associate Professor with the School of Navigation, Wuhan University of Technology. His research interests include ship navigation information system and data transmission processing and traffic environment and safety assurance.



ZHAO LIU received the Ph.D. degree in traffic information engineering and control from the Wuhan University of Technology, in 2017. His research interests include modeling and simulation of water transportation systems, maritime big data mining and visual analysis, and safety evaluation of water transportation systems.



SHUZHE CHEN received the M.Sc. and Ph.D. degrees from the Wuhan University of Technology, in 2006 and 2012, respectively. He is currently an Associate Professor with the School of Navigation, Wuhan University of Technology. He has published more than 30 scientific papers in international journals and conferences. His research interests include risk navigation and accident playback inversion.



BIAO GONG received the B.S. degree from the Wuhan University of Technology, where he is currently pursuing the M.Sc. degree in transport engineering. His research interests include risk navigation and accident playback inversion.



RUI WANG received the M.Sc. degree from the Wuhan University of Technology, in 2020. She is currently an Engineer with Wuhan Hai Zhi Cheng Technology Company Ltd. Her research interests include safety engineering and green shipping.

...